Enhancement of the dielectric constant near a percolation threshold

David Wilkinson, J. S. Langer,* and Pabitra N. Sen
Schlumberger-Doll Research Center, P.O. Box 307, Ridgefield, Connecticut 06877
(Received 19 November 1982)

When one of the components of a mixture of two materials is a conductor, geometrical effects can lead to a dielectric constant for the mixture which is much greater than that of either constituent. Here we illustrate a simple example of this effect in a two-dimensional network consisting of randomly placed conductors and capacitors. The dielectric enhancement is obtained as a function of frequency and the concentration of conductors. The calculational technique used is the position-space renormalization group in which smaller units are combined iteratively to form larger units.

I. INTRODUCTION

The low-frequency dielectric constant ϵ' of brine-saturated porous media can be large due to geometrical as well as electrochemical effects.[1,2] One possible explanation of this phenomenon is to make an analogy with the well-known dielectric enhancement which occurs in inhomogeneous mixtures of metals and insulators when the conducting metallic phase is close to percolation threshold.[3–6] Notable progress has been made for such systems in developing scaling theories to predict the behavior of the conductivity σ and the dielectric constant ϵ' as functions of the volume fraction ϕ of the conducting material and the frequency ω. Results of interest here predict that the low-frequency conductivity vanishes at the percolation threshold ϕ_c according to a power law of the form

$$\sigma \sim \sigma_w(\phi-\phi_c)^t, \quad \phi>\phi_c$$
$$\sigma=0, \quad \phi<\phi_c \tag{1.1}$$

where σ_w is the conductivity of the conducting phase, which is the water in the case of brine-saturated porous media. The real part of the dielectric constant is predicted to diverge as ϕ approaches (from below or above) ϕ_c

$$\epsilon' \sim \epsilon'_m \mid \phi-\phi_c \mid^{-s}, \tag{1.2}$$

where ϵ'_m is the dielectric constant of the matrix. The above results (1.1) and (1.2) hold for low frequencies

$$\omega \ll \mid \phi-\phi_c \mid^{s+t} \frac{\sigma_w}{\epsilon'_m \epsilon_0}, \tag{1.3}$$

where ϵ_0 is the permittivity of the vacuum.

For $\omega \gg \mid \phi-\phi_c \mid^{(s+t)} \sigma_w/\epsilon'_m\epsilon_0$, the dielectric constant ϵ' increases as frequency is lowered,

$$\epsilon' \sim \epsilon'_m \left[\frac{\sigma_w}{\epsilon'_m \epsilon_0 \omega}\right]^{s/(s+t)}. \tag{1.4}$$

In the scaling laws (1.1), (1.2), and (1.4), the exponents t and s are the usual conductivity and superconductivity exponents.[7] These exponents are universal for random systems, i.e., they do not depend on details of the geometry such as grain shape or coordination number, but only on the space dimension of the system. (Note, however, that correlations in the geometry will, in general, change the exponents.) Best values at present are $s=t\sim 1.3$ in two dimensions and $s\sim 0.7$ and $t\sim 1.8$ in three dimensions.[8]

Although these general results are well known, it would seem of interest to illustrate this phenomenon within a particular calculational scheme. The position-space renormalization-group (PSRG) method has been found useful in computing approximate values for critical exponents of the above kind for magnetic systems, resistor networks, etc.,[9–12] but has not so far been used to calculate electrical properties of continuous media. It is known that PSRG treats statistical fluctuations more carefully than the effective-medium theories that we have developed previously,[1] and thus should give reasonable results both inside and outside the critical region $\phi\sim\phi_c$, $\omega\sim 0$ described above. In preparation for an extension of PSRG to the continuum situation, we apply this method to the simplest network model which has some relevance to dielectric enhancement in porous media, i.e., a capacitor-resistor network, with the capacitors representing the insulating rock grains and the resistors the conducting water. Such a network model may be used, in principle, to simulate the continuum by taking ever smaller sizes of elements. But what is more important is that the network model shares many essential geometrical features with the continuum, such as tortuosity and interruption of a long conductive path by a thin nonconducting zone.

In Sec. II we describe the two-dimensional network model and the position-space renormalization-group approximation. We consider the simplest possible rescaling, i.e., the collapsing of a 2×2 cell. The renormalized conductivities are approximated by a bimodal distribution in which all elements are classified as capacitive or conductive. Both the linearized and the full nonlinear recursion relations are considered. The former give the exponents of the scaling laws near the critical point. The latter provide a useful computational scheme away from the critical point where simple scaling laws are no longer valid. In Sec. III we compare our results with another approximate method—effective-medium theory. Finally in Sec. IV, we summarize our results and discuss their possible application to the case of fluid-saturated porous media.

II. THE POSITION-SPACE RENORMALIZATION-GROUP APPROXIMATION

The model that we wish to consider is a regular, two-dimensional, square network consisting of two kinds of randomly placed conductances, g_1 and g_2, as shown in Fig. 1. The element $g_1=\sigma$ is purely resistive and occurs with probability p. The second element is purely capacitive, $g_2=i\omega c$, and occurs with probability $q=1-p$. The

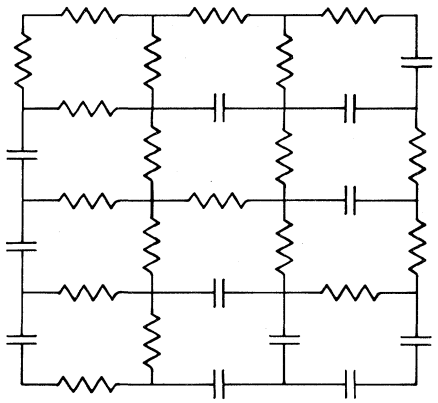

FIG. 1. Resistor-capacitor network. Each bond is occupied randomly by a conductor $g_1=\sigma$ with probability p, or a capacitor $g_2=i\omega c$ with probability $1-p$.

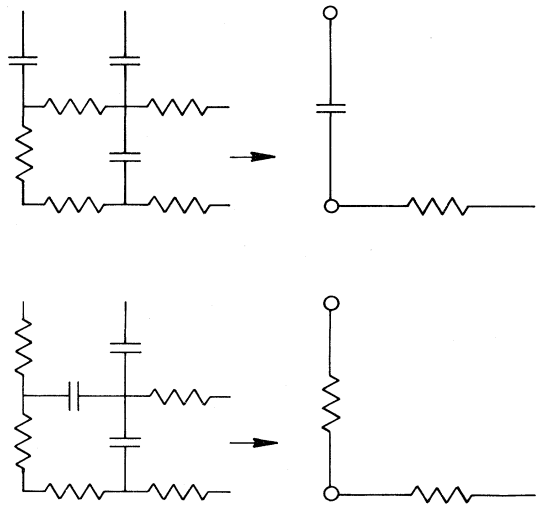

FIG. 2. Two examples of a renormalization transformation in the bimodal approximation. Each cell is collapsed into conductive or capacitative elements in the vertical and horizontal directions.

problem is to compute the complex conductance of a very large sample of this network.

Our strategy is to start with a position-space renormalization group in which bigger cells are collapsed into smaller cells as shown in the diagram of Fig. 2. This model is known to produce a reasonably good solution of the bond-percolation problem on the square lattice. Even this relatively simple scheme, however, cannot be carried out in detail for our problem, and we shall have to resort to a crude truncation approximation. The difficulty is that distributing g_1 and g_2 on the bonds of the diagram in all possible arrangements with appropriate statistical weights produces a complicated new distribution of complex conductances after one renormalization transformation. In principle, this transformation should be iterated indefinitely many times in order to perform a correct renormalization-group calculation. It is possible that the full functional formulation of this problem can be solved exactly, but we do not propose to attempt such a treatment here. Rather, we shall simply approximate the new distribution by one in which all the weight is again concentrated at two new complex values of the conductances, g_1' and g_2', with probabilities p' and $q'=1-p'$, respectively, as shown in Fig. 2. For convenience, we shall continue to refer to g_1 as the conductor and g_2 as the capacitor, even when both conductances have become complex. In our renormalization prescription, we treat the conductivity in the vertical and horizontal directions independently; since these directions are equivalent we may consider just the vertical case. If we apply "bus bars" to the top and bottom of the diagram (see Fig. 2), the effective conductance is determined by just five circuit elements in a Wheatstone-bridge arrangement, so there are $2^5=32$ possible configurations. We divide these configurations into two groups: "conducting" diagrams in which the component g_1 forms a conducting path, and "insulating" where it does not. The renormalized occupation probability p' is the sum of the probabilities of the conducting diagrams, and the renormalized value g_1' is the weighted arithmetic mean of the corresponding conductances in the vertical direction. Similarly, the new value of g_2' is the weighted mean of the insulating diagrams. This special grouping makes good sense when, for example, $|g_2| \ll |g_1|$, so that the conductances of the various configurations are distributed almost bimodally with either large values near g_1' or small values near g_2'. For this reason the validity of our results is limited to the frequency regime $\omega<\sigma/c$; in principle the region $\omega>\sigma/c$ may be probed by interchanging the roles of g_1 and g_2, but we shall not do this here.

Using the above presciption, we obtain a renormalization transformation of the form

$$p'=f(p)\ ,\quad p'g_1'=g_1f_1(p,\alpha)\ ,\quad q'g_2'=g_2f_2(p,\alpha)\ , \tag{2.1}$$

where $\alpha=g_2/g_1$, and

$$f(p)=p^5+5p^4q+8p^3q^2+2p^2q^3\ , \tag{2.2}$$

$$f_1(p,\alpha)=p^5+p^4q+4p^4q\left[\frac{3+5\alpha}{5+3\alpha}\right]+2p^3q^2\left[\frac{1+\alpha}{2}\right]+4p^3q^2\left[\frac{1+5\alpha+2\alpha^2}{2+5\alpha+\alpha^2}\right]+2p^3q^2\left[\frac{1+3\alpha}{3+\alpha}\right]+2p^2q^3\left[\frac{1+\alpha}{2}\right]\ , \tag{2.3}$$

$$f_2(p,\alpha)=q^5+pq^4+4pq^4\left[\frac{5+3\alpha}{3+5\alpha}\right]+2p^2q^3\left[\frac{2}{1+\alpha}\right]+4p^2q^3\left[\frac{2+5\alpha+\alpha^2}{1+5\alpha+2\alpha^2}\right]+2p^2q^3\left[\frac{3+\alpha}{1+3\alpha}\right]+2p^3q^2\left[\frac{2}{1+\alpha}\right]\ . \tag{2.4}$$

It is convenient to combine (2.1), (2.3), and (2.4) into a single relation of the form

$$\frac{\alpha'}{\alpha}=\frac{p'f_2(p,\alpha)}{q'f_1(p,\alpha)}\ , \tag{2.5}$$

so that (2.2) and (2.5) define flows in the space of three parameters: p, Reα, and Imα.

To begin an analysis of these recursion relations, consider the flows in the case where both g_1 and g_2 are purely resistive elements with real conductances. The flow diagram is shown in Fig. 3. Note that there are six fixed points shown in this figure, at $p=0$, $\frac{1}{2}$, and 1 with $\alpha=0$ or 1. The unstable fixed point at $p=\frac{1}{2},\alpha=0$ corresponds to the critical percolation threshold; in fact, $p_c=\frac{1}{2}$ is the exact percolation threshold for a two-dimensional square network.

System points which start with p greater than p_c and sufficiently small α flow directly towards the line $p=1$ with only little initial change in α. This means that the distribution remains bimodal, at least for a large number of iterations, but that the statistical weight becomes concentrated at the value of g_1, which becomes the effective conductance $g_{\rm eff}$ as p approaches unity. Similarly, when p is initially less than p_c and α is small, the system point flows towards $p=0$. The distribution again remains bimodal, but the smaller conductance, the transformed value of g_2, becomes overwhelmingly the most probable. In the case $\alpha=0$ the system is effectively an insulator. The use of this kind of transformation at $\alpha=0$ to discuss the insulating to conducting transition has been described extensively in the literature.[9–11]

Another notable feature of the flow pattern in Fig. 3 is that system points which start near $p=p_c$ with appreciable values of α move directly toward $\alpha=1$ with relatively little initial change in p. In this case g_1 and g_2 become equal, and the effective conductance $g_{\rm eff}$ is this common value. Although in this case it no longer makes sense to consider a bimodal distribution of conductances, this does not really matter since once α becomes close to unity, we see from (2.3) and (2.4) that g_1 and g_2 remain constant.

Eventually all system points slow to one of the points $\alpha=1$, $p=0$ or 1, which are the only fully stable fixed points of the diagram. In the complex α plane, the flows are, of course, more complicated, but qualitatively they are the same; in particular the system always flows to $\alpha=1$, with $p=0$ or 1. The crossover between the two different ways these points can be approached, as described above for the real case, will, in what follows, be the key to understanding the dielectric enhancement.

We will first compute the scaling properties in the critical region by linearizing the recursion relations around the unstable fixed point $p=p_c=\frac{1}{2}$, $\alpha=0$. We have

$$p'-p_c\cong r(p-p_c)\ ,\quad r=\tfrac{13}{8} \tag{2.6}$$

$$g_1'/g_1=2f_1(\tfrac{1}{2},\alpha)\cong a_1+b_1\alpha+\cdots\ ,\quad a_1=\tfrac{17}{30} \tag{2.7}$$

$$g_2'/g_2=2f_2(\tfrac{1}{2},\alpha)\cong a_2+b_2\alpha+\cdots\ ,\quad a_2=\tfrac{23}{12} \tag{2.8}$$

$$\frac{\alpha'}{\alpha}=\frac{f_2(\frac{1}{2},\alpha)}{f_1(\frac{1}{2},\alpha)}=A+B\alpha+\cdots\ ,\quad A=\frac{a_2}{a_1}=\tfrac{115}{34}\ . \tag{2.9}$$

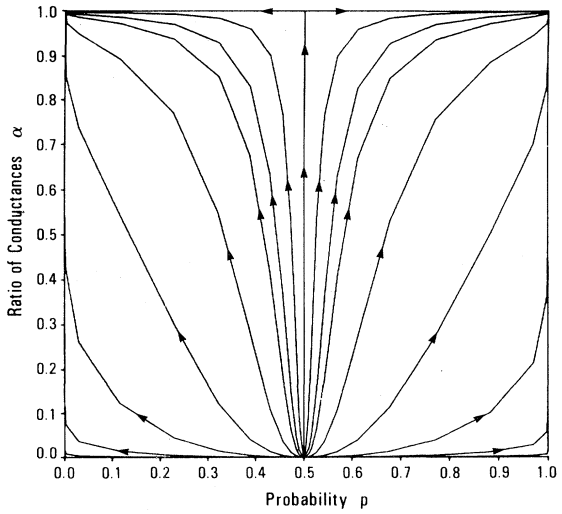

FIG. 3. Renormalization-group flows in the real case. The point $p=\frac{1}{2}$, $\alpha=0$ is the unstable fixed point. All points flow to $\alpha=1$ with $p=0$ or 1.

Let us start by considering p slightly larger than p_c and, now, let us consider small but complex values of α. That is, we revert to our original problem in which the initial value of α is $i\omega c/\sigma$, and we consider very small frequencies ω. From (2.6) we deduce that the flow reaches the vicinity of $p=1$ after n iterations, where $n\sim\ln(1/2\Delta p)/\ln(r)$ and $\Delta p=p-p_c$. At this point, the transformed conductance $g_1(n)$ gives us the effective conductance $\sigma_{\rm eff}$:

$$\sigma_{\rm eff}\sim g_1(n)\sim a_1^n\sigma\sim\sigma(\Delta p)^t\ , \tag{2.10}$$

with $t=-(\ln a_1)/(\ln r)\sim 1.17$. This is the lattice analog of (1.1).

Equation (2.9) is now useful for checking the validity of this approximation, that is, for seeing whether α actually remains small through n iterations. In terms of the flow diagram of Fig. 3, this corresponds to systems which approach the fixed point at $p=1,\alpha=1$ by first moving to the right and then upward. Then nth iterate of α is

$$\begin{aligned}\alpha(n)&=\frac{i\omega c}{\sigma}\prod_{m=0}^{n-1}[A+B\alpha(m)]\\&\sim\frac{i\omega c}{\sigma}A^n\left[1+\frac{B}{A}\sum_{m=0}^{n-1}\alpha(m)\right]\\&\sim\frac{i\omega c}{\sigma}A^n\left[1+\frac{i\omega c}{\sigma}\frac{B}{A}\frac{(A^n-1)}{(A-1)}\right]\ ,\end{aligned} \tag{2.11}$$

where we have used $\alpha(m)\sim i\omega c/\sigma A^m$ in evaluating the bracketed terms. At this level of approximation the criterion $|\alpha(n)|\ll 1$ becomes

$$\frac{i\omega c}{\sigma}A^n\ll 1$$

or

$$\omega\ll\omega_c\equiv\frac{\sigma}{c}(\Delta p)^{t+s}\ , \tag{2.12}$$

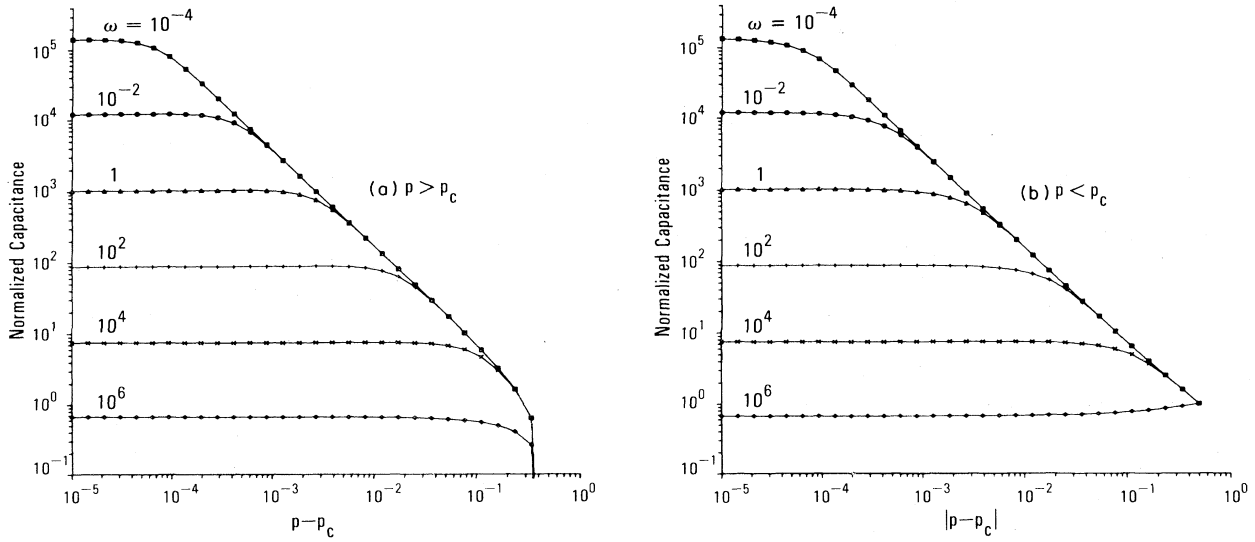

FIG. 4. Variation of $c_{\rm eff}$ with p for various ω, showing the critical behavior and crossover. The quantity plotted is the normalized capacitance $c_{\rm eff}/c$. For $\omega > 10^6$ the results break down because $\omega c/\sigma > 1$.

where $s=(\ln a_2)/(\ln r)=1.34$, and t is the same as in (2.10). (Actually in two dimensions there is a dual symmetry which implies that s and t are rigorously equal.[13,14] Our truncation scheme violates this symmetry[15] and hence gives unequal, though comparable, values for these exponents. Hopefully this discrepancy would be reduced by considering larger cells.) Equation (2.12) shows that the range of ω values for which (2.10) is valid vanishes as p approaches p_c.

Within the range of validity described by (2.12), we can use the approximate procedure summarized in (2.11) to compute an effective capacitance $c_{\rm eff}$. To do this, we improve (2.10) by keeping the second term in (2.7),

$$g_{\rm eff}\sim\sigma\prod_{m=0}^{n-1}[a_1+b_1\alpha(m)]$$
$$\sim\sigma a_1^n\left[1+\frac{i\omega c}{\sigma}\frac{b_1}{a_1}\frac{(A^n-1)}{(A-1)}\right]. \tag{2.13}$$

This implies that

$$c_{\rm eff}\equiv\frac{1}{\omega}\,{\rm Im}(g_{\rm eff})\sim c(\Delta p)^{-s}, \tag{2.14}$$

where the exponent s was defined in (2.12). This is result (1.2) of the Introduction. Note that $c_{\rm eff}$ diverges as p approaches p_c at zero frequency ω, but that, at any nonzero frequency, the formula loses its validity as $p\to p_c$ because of the restriction (2.12).

The identical analysis can be repeated in the insulating region $p<p_c$. Now the probability flows to $p=0$, so that $g_{\rm eff}$ must be computed from the iterated value of g_2. The effective capacitance diverges as $\Delta p\to 0$ in the same way as for $p>p_c$:

$$c_{\rm eff}\sim c\,|\,\Delta p\,|^{-s}, \tag{2.15}$$

while for the conductivity we obtain the new result

$$\sigma_{\rm eff}\sim\frac{\omega^2c^2}{\sigma}\,|\,\Delta p\,|^{-(t+2s)}. \tag{2.16}$$

The region of validity of (2.15) and (2.16) is the same as for (2.10) and (2.14) except that Δp in (2.12) becomes $|\,\Delta p\,|$. It is interesting to note that using either (2.10) and (2.14) or (2.15) and (2.16) that the cutoff frequency ω_c in (2.12) may be interpreted as that frequency for which the effective resistance-capacitance constant $c_{\rm eff}/\sigma_{\rm eff}$ is of order $1/\omega$.

It remains to be seen how our renormalization-group procedure can be used to calculate the complex conductance in the frequency region above ω_c, that is, where $1>\omega c/\sigma\gg|\,\Delta p\,|^{t+s}$. Within the linearized approximation, the two conductances never become equal because g_1 remains real while g_2 remains imaginary, but we may estimate the number of iterations for the full nonlinear map to reach $\alpha=1$ by computing the number of iterations n^* for which the absolute value of $\alpha(n^*)$ becomes of order unity. From (2.9) we see that this gives $n^*\sim-\ln(\omega c/\sigma)/\ln A$, so that

$$g_{\rm eff}\sim a_1^{n^*}\sigma\sim\sigma\left[\frac{\omega c}{\sigma}\right]^{t/(t+s)}. \tag{2.17}$$

Since the full nonlinear map would generate an imaginary part of similar magnitude, we see that the effective capacitance is given by

$$c_{\rm eff}\equiv\frac{1}{\omega}\,{\rm Im}g_{\rm eff}\sim c\left[\frac{\omega c}{\sigma}\right]^{-s/(s+t)}. \tag{2.18}$$

This is result (1.4) of the Introduction. Our approximate computation gives $s/(s+t)=0.53$; the exact result in two dimensions would yield $\frac{1}{2}$ for this exponent, since s and t are equal.

Perhaps the greatest advantage of this scheme is that it

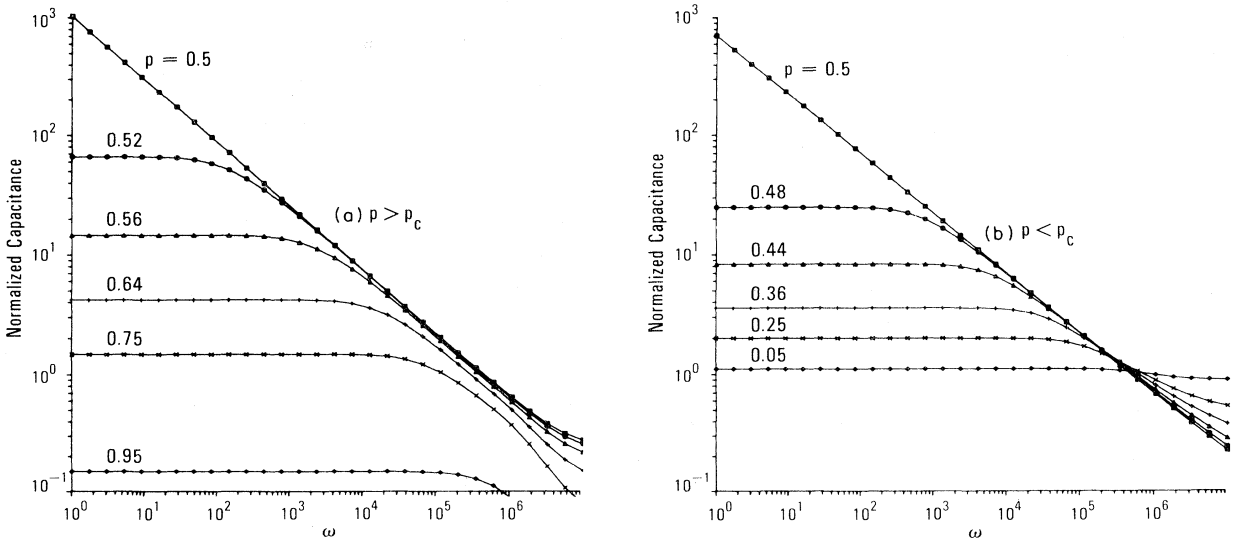

FIG. 5. Variation of c_{eff} with ω for various p, similar to Fig. 4.

can be used to compute numerical approximations to the complex conductance at values of p and ω which are finite distances away from the critical point, $p=p_c=\frac{1}{2}$, $\omega=0$. In principle, this means that the technique might be used in a practical way for more realistically complicated models. To perform such calculations, we start with a given occupation probability p and initial physical values of $g_1=\sigma$ and $g_2=i\omega c$, and directly iterate the nonlinear recursion relations (2.1). All initial states with nonvanishing ω eventually flow to $\alpha=1$ in the nonlinear theory, so there is no difficulty in identifying g_{eff} as the unique limit of the iteration process, even when the bimodal distribution persists out to $p=0$ or $p=1$.

Some actual results are shown in Figs. 4 and 5 for the case $\sigma=1\ \Omega^{-1}$ and $c=1\ \mu$F. The effective conductance and capacitance are defined as $\sigma_{\text{eff}}=\text{Re}(g_{\text{eff}})$ and $c_{\text{eff}}=\text{Im}(g_{\text{eff}})/\omega$. Since we are primarily concerned with the dielectric enhancement, we will present results only for c_{eff}. In Fig. 4 this quantity is shown as a function of p for various values of ω, while in Fig. 5, it is shown as a function of ω for various values of p. The enhancement of c_{eff} near $p=p_c$ and $\omega=0$ appears clearly, as does the p-dependent crossover between high- and low-frequency regimes.

III. COMPARISON WITH OTHER MODELS

It is interesting to compare these results with those which would be obtained in an effective-medium treatment. In the coherent-potential approximation (CPA) the complex conductance is given by[16]

$$g_{\text{eff}}=\sigma[x+(x^2+\alpha)^{1/2}]\ , \tag{3.1}$$

with

$$x=(p-\tfrac{1}{2})(1-\alpha)\ . \tag{3.2}$$

In the present case of a two-dimensional square network, the effective-medium formula gives the correct percolation threshold $p_c=\frac{1}{2}$, and also reproduces the results (2.10) and (2.14)–(2.16) with the exponents taking the values $s=t=1$. In Fig. 6 the effective capacitance $c_{\text{eff}}=\text{Im}(g_{\text{eff}})/\omega$ is plotted as a function of frequency ω. The results are qualitatively similar to the results for PSRG in Fig. 5. The CPA does unusually well in this problem; in general, one would expect PSRG to treat the critical region better than CPA. This would become more apparent in three dimensions, where CPA still gives $s=t=1$ compared to the correct values $s\sim 0.7$ and $t\sim 1.8$. In the dilute limits $p\to 0$ or 1, however, it is known that CPA is exact. In the limit $p\to 0$ we find from (3.1)

$$g_{\text{eff}}=i\omega c\left[1+2p\frac{1-\alpha}{1+\alpha}\right]+O(p^2)\ , \tag{3.3a}$$

so that at low frequency

$$c_{\text{eff}}=c(1+\lambda p)\ , \tag{3.3b}$$

$$\sigma_{\text{eff}}=\mu p\frac{\omega^2c^2}{\sigma}\ , \tag{3.3c}$$

with $\lambda=2$ and $\mu=4$. Similarly as $p\to 1$

$$g_{\text{eff}}=\sigma\left[1-2q\frac{1-\alpha}{1+\alpha}\right]+O(q^2)\ , \tag{3.4a}$$

and at low frequency

$$c_{\text{eff}}=\mu qc\ , \tag{3.4b}$$

$$\sigma_{\text{eff}}=\sigma(1-\lambda q)\ , \tag{3.4c}$$

again with $\lambda=2$ and $\mu=4$. In our PSRG formulation the corresponding result as $p\to 0$ is

$$g_{\text{eff}}=i\omega c\left[1+8p\frac{1-\alpha}{3+5\alpha}\right]+O(p^2)\ , \tag{3.5}$$

so that the low-frequency capacitance and conductivity are as in (3.3) but with $\lambda=\frac{8}{3}$ and $\mu=\frac{64}{9}$. Similarly as $p\to 1$, PSRG gives

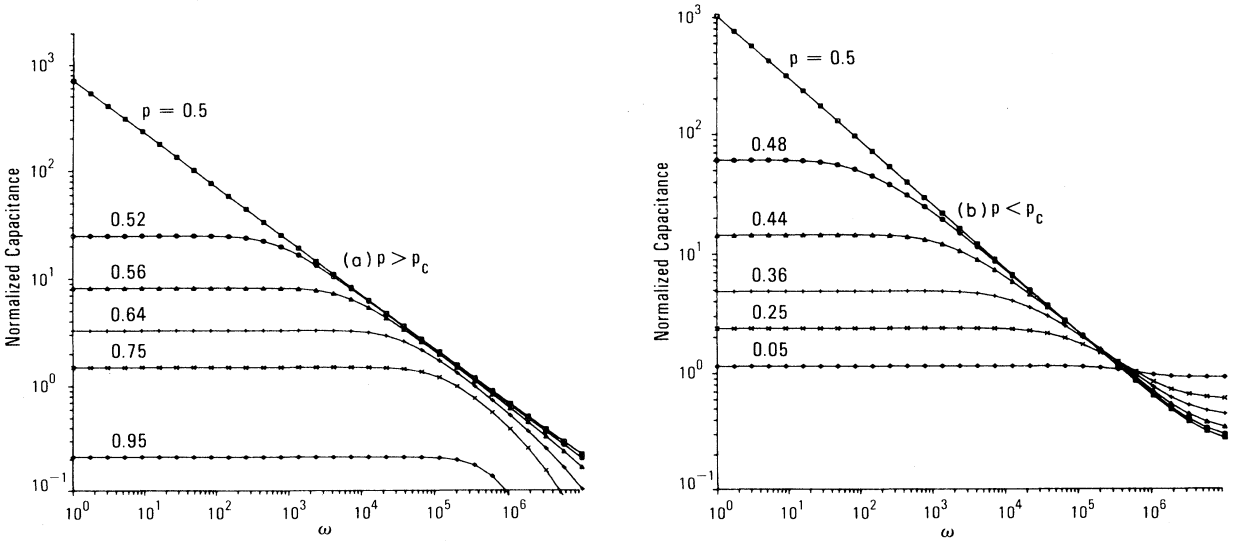

FIG. 6. Effective-medium prediction for variation of c_{eff} with ω for various p.

$$g_{\text{eff}}=\sigma\left[1-8q\frac{1-\alpha}{5+3\alpha}\right]+O(q^2)\ , \tag{3.6}$$

so that the low-frequency results are as in (3.4) but with $\lambda=\frac{8}{5}$ and $\mu=\frac{64}{25}$.

We see that PSRG correctly predicts the linear dependence on the concentration in the dilute limits, but that the slopes are not exact. This discrepancy is due to our truncation procedure. As shown by Bernasconi,[11] if one keeps the full distribution of conductances and corresponding probabilities at each step, and identifies g_{eff} as the weighted average, then for a 2×2 cell the iterated result converges to the exact result (3.3) or (3.4) in the dilute limits. While this method can be implemented as a computational scheme outside the dilute regimes, it becomes extremely cumbersome owing to the large number of conductances generated after a few iterations.

Bernasconi[11] also suggests a different truncation scheme in which the transformed conductances g_1' and g_2' are identified as the *geometric* means of the conducting and nonconducting diagrams, rather than the *arithmetic* means used in this paper. This truncation has the advantage that it respects the dual symmetry of the square lattice.[13–15] Thus in the critical region the exponents s and t are automatically equal, and in fact take the common value

$$s=t=\frac{\ln(400/3)}{8\ln(13/8)}=1.26\ . \tag{3.7}$$

In the dilute limits the results are also more symmetrical; the low-frequency results corresponding to (3.3) and (3.4) are obtained in both cases by replacing λ and μ by $4\ln(\frac{5}{3})$ and $\frac{64}{15}$, respectively. Here again the slopes deviate from the exact results because of the bimodal approximation.

IV. DISCUSSION

In this paper we have investigated a purely geometrical mechanism for low-frequency enhancement of the dielectric constant in systems containing mixtures of conductors and dielectrics. As a concrete example, we have considered a two-dimensional capacitor-resistor network, in which conductance and capacitance of the network play the role of conductivity and dielectric constant of the medium. With the use of the position-space renormalization-group method, the capacitance was obtained as a function of frequency and concentration of conductors.

It should be noted that the dielectric constant discussed in this work, as well as in the previous work cited in the Introduction, is that at zero wave number k, i.e., the quantity $\epsilon(\omega)=\lim_{k\to0}\epsilon(k,\omega)$. It has also been assumed throughout that the frequency is sufficiently low for a quasistatic treatment to be correct. In comparison with real experiments it is important to check that this condition is being met.

The motivation for this work was the phenomenon of dielectric enhancement in porous rocks containing salty, i.e., conducting, water. Although a low-frequency dielectric enhancement is indeed observed in such rocks, the results described in this paper strictly refer only to a random system. Such a system always exhibits a non zero percolation threshold ϕ_c below which the dc conductivity vanishes. In reality, however, the empirical law known as Archie's Law

$$\sigma\sim\sigma_w\phi^m\ , \tag{4.1}$$

indicates that $\phi_c=0$, i.e., the water in the pore space remains conducting down to arbitrarily low concentrations. If we assume that the pore space is completely filled with water, this means geometrically that the pore space remains connected even in samples with very low porosity. The extension of PSRG to such correlated geometries is an interesting and important problem.

One of the key properties of the dielectric enhancement for random systems is the universal behavior in the critical region. Presumably, the analog for rocks of the limit $\phi\to\phi_c$ is the low porosity limit. Although a corresponding universality would explain the wide applicability of Archie's law with $m\sim2$, it remains to be proved that such

universality exists with respect to variations such as grain shape and packing geometry. Indeed in one class of model, the iterated effective-medium approximation,[17–19] there is only weak dielectric enhancement and the exponent m depends on grain shape. In the language of this paper, s is zero and t is nonuniversal; for the case of a two-dimensional square network, one finds $t=2$ and $s=0$. Although the iterated effective-medium approximation is carefully constructed to give a zero percolation threshold, the exponents are controlled by the dilute rock limit, and it is not clear that the results are valid in the low porosity regime where the rock grains are touching. It would be extremely useful for geophysical prospecting if there did exist universal laws governing dielectric enhancement for the case of fluid-saturated porous media.

ACKNOWLEDGMENT

The authors would like to thank S. Redner and D. L. Johnson for useful discussions.

*Permanent address: Institute for Theoretical Physics, Santa Barbara, California 93106.

[1]P. N. Sen, Appl. Phys. Lett. 39, 667 (1981); Geophysics 46, 1417 (1981).

[2]W. C. Chew and P. N. Sen, J. Chem. Phys. 77, 4683 (1982).

[3]A. L. Efros and B. I. Shklovskii, Phys. Status Solidi B 76, 475 (1976).

[4]D. Stroud and D. Bergman, Phys. Rev. B 25, 2061 (1982).

[5]D. M. Granan, J. C. Garland, and D. B. Tanner, Phys. Rev. Lett. 46, 375 (1981).

[6]I. Webman, J. Jortner, and M. H. Cohen, Phys. Rev. B 16, 2593 (1982).

[7]J. P. Straley, J. Phys. C 9, 783 (1976).

[8]For a recent compilation of conductivity exponents, see A. B. Harris (unpublished).

[9]J. P. Straley, J. Phys. C 10, 1903 (1977).

[10]S. Kirkpatrick, in *Ill Condensed Matter,* edited by R. Balian, R. Maynard, and G. Toulouse (North-Holland, Amsterdam, 1979).

[11]J. Bernasconi, Phys. Rev. B 18, 2185 (1978).

[12]P. J. Reynolds, H. E. Stanley, and W. Klein, Phys. Rev. B 21, 1223 (1980), and references therein.

[13]A. M. Dykhne, Zh. Eksp. Teor. Fiz. 59, 110 (1970) [Sov. Phys.—JETP 59, 111 (1970)].

[14]J. Marchant and R. Gallibard, C. R. Acad. Sci. Ser. B 281, 261 (1975).

[15]The reason our scheme violates the dual symmetry is that in the duality theorem (Refs. 13 and 14) the conductances of the dual system are the reciprocals of the original ones, and this relation is not preserved under taking of arithmetic means. The duality is maintained if one takes arithmetic means for the conducting diagrams and harmonic means for the insulating ones (or vice versa) or, as suggested by Bernasconi (Ref. 11), if one takes geometric means in both cases.

[16]S. Kirkpatrick, Rev. Mod. Phys. 45, 574 (1973).

[17]P. N. Sen, C. Scala, and M. H. Cohen, Geophysics 46, 781 (1981).

[18]K. S. Mendelson and M. H. Cohen, Geophysics 47, 257 (1982).

[19]P. N. Sen (unpublished).